Role of the N-Terminus of Epidermal Growth Factor in ErbB-2/ErbB-3 Binding Studied by Phage Display†

Catelijne Stortelers,‡ Christelle Souriau,§,|| Ellis van Liempt,‡ Monique L. M. van de Poll,‡ and Everardus J. J. van Zoelen*,‡

Department of Cell Biology, University of Nijmegen, Toernooiveld 1, 6525 ED Nijmegen, The Netherlands, and IGM-CNRS, UMR 5535, 1919 Route de Mende, 34293 Montpellier Cedex 35, France

Received March 27, 2002; Revised Manuscript Received May 15, 2002

ABSTRACT: Epidermal growth factor (EGF) binds with high affinity to the EGF receptor, also known as ErbB-1, but upon replacement of the N-terminal linear region by neuregulin (NRG) 1 or transforming growth factor (TGF) α sequences it gains in addition high affinity for ErbB-2/ErbB-3 heterodimers. However, these chimeras weakly bind to ErbB-3 alone. To further dissect the ligand binding selectivity of the ErbB network, we have applied the phage display technique to examine the role of the linear N-terminal region in EGF for interaction with ErbB-2/ErbB-3 heterodimers. A library of EGF variants was constructed in which residues 2, 3, and 4 were randomly mutated, followed by selection for binding to intact MDA-MB-453 cells that overexpress ErbB-2 and ErbB-3 but lack ErbB-1. Analysis of the selected phage EGF variants revealed clones with high binding affinity to ErbB-2/ErbB-3 while maintaining high affinity to ErbB-1. In these variants, Trp (or alternatively His) was almost exclusively present at position 2, while specific combinations of hydrophobic, basic, and small residues were found at positions 3 and 4. The mitogenic activity of the phage EGF variants corresponded with their relative binding affinity. Two of the selected EGF variants, EGF/WVS and EGF/WRS, were further characterized as recombinant proteins. In contrast to previously characterized chimeras of EGF with NRG-1 or TGF-α, these variants did not only show high binding affinity for ErbB-2/ErbB-3 heterodimers but also for ErbB-3 alone. These data show that the linear N-terminal region of EGF-like growth factors is directly involved in binding to ErbB-3.

The ErbB family of receptor tyrosine kinases includes the epidermal growth factor receptor (EGFR or ErbB-1), ErbB-2 (or Neu), ErbB-3, and ErbB-4. Activation of the intrinsic kinase activity occurs upon ligand binding and subsequent receptor dimerization, during which both homodimeric and heterodimeric receptor complexes can be formed. ErbB receptors play an important role in oncogenesis, particularly as a result of their overexpression in many epithelial tumor cells (*1*, *2*). Moreover, the ErbB signaling network is currently one of the most direct targets in the development of antitumor drugs.

Soluble ligands for mammalian ErbB receptors can be divided into three groups depending on their receptor selectivity. The growth factors EGF,[1] transforming growth factor (TGF) α and amphiregulin specifically bind ErbB-1, while betacellulin, epiregulin, and heparin-binding EGF-like growth factor can interact with both ErbB-1 and ErbB-4. Finally, the numerous isoforms of neuregulins (NRG) 1−4 specifically bind to ErbB-3 and/or ErbB-4 (*3*−*5*). No soluble ligand has yet been identified for the ErbB-2 receptor.

All ligands share a conserved structural EGF-like motif of around 50 amino acids, characterized by six conserved cysteines and two glycines which define a three-looped structure (A-, B-, and C-loop, respectively) with flexible N- and C-terminal linear regions. Structural analysis of human EGF revealed a major antiparallel β-sheet in the B-loop region and a minor antiparallel β-sheet in the C-loop (*6*, *7*). Although several ligands contain extended sequences at the N- and C-terminal ends, the EGF domain of ErbB ligands is sufficient for receptor activation. Receptor binding specificity of EGF-like growth factors is achieved by the presence of amino acids that facilitate binding to a specific ErbB receptor in addition to amino acids that impair interaction with other ErbB members (*8*). In the case of EGF, both mutational and structural studies have indicated that residues surrounding the second and sixth conserved cysteines, including Tyr13, Leu15, His16, Tyr37, Arg41, and Leu47, are crucial for binding to ErbB-1, presumably by forming a nonlinear binding domain (see Figure 1). While substitutions in the B-loop region were also found to affect ErbB-1 binding, its role is controversial, and this region is believed

† This work was supported by Grant KUN-97-1387 from the Dutch Cancer Society (KWF) and by a fellowship from Stichting De Drie Lichten.

* Corresponding author. Phone: ++31 24 3652707. Fax: ++31 24 3652999. E-mail: vzoelen@sci.kun.nl.

‡ University of Nijmegen.

§ IGM-CNRS.

|| Current address: CSIRO HSN, 343 Royale Parade, Parkville, Victoria 3052, Australia.

[1] Abbreviations: BSA, bovine serum albumin; DF, 1:1 mixture of DMEM and Ham's F12 medium; DMEM, Dulbecco's modified Eagle's medium; EGF, epidermal growth factor; FCS, fetal calf serum; IL, interleukin; NRG, neuregulin; PBS, phosphate-buffered saline; SDS−PAGE, sodium dodecyl sulfate−polyacrylamide electrophoresis; TGF, transforming growth factor; tu, titrating unit.

10.1021/bi025878c CCC: $22.00
Published on Web 06/12/2002

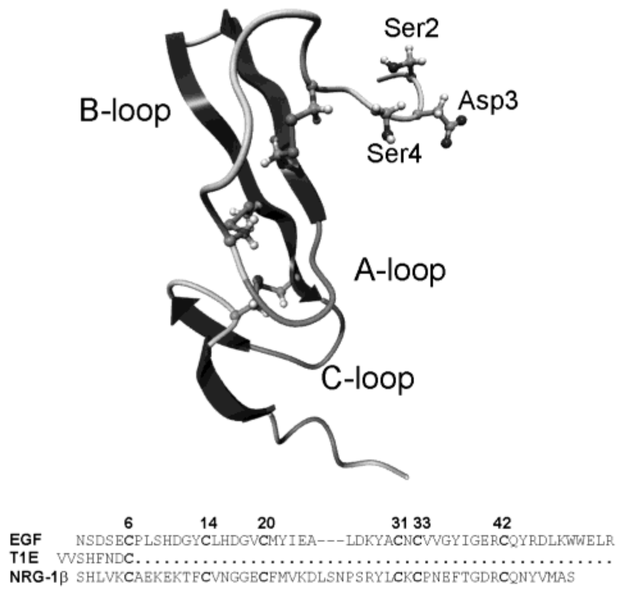

FIGURE 1: Structure and sequence of EGF and related molecules. Representation of the hEGF structure showing the relative positions of Ser2, Asp3, and Ser4 randomized in the EGF/234 library and the three disulfide bridges formed by the six conserved cysteines. The figure was generated from the NMR coordinates of egf28 (PDB) available at www.ocms.ox.ac.uk/idc/structures/egf (*6*). The alignment of the sequences of human EGF, the chimera T1E, and human NRG-1$\beta_{177-226}$ is given with numbering of the conserved cysteines in bold face according to EGF.

to serve primarily as a scaffold for maintaining the proper conformation (*6*, *9*−*12*). By contrast, a combination of alanine scanning and structural analysis has shown that binding of NRG-1 to ErbB-3 involves a set of hydrophobic residues clustered in the linear N-terminal region and the B-loop (*13*, *14*), suggesting that EGF-like growth factors may use distinct regions for binding to different ErbB receptors. Further evidence for an important role of the linear N-terminal region of EGF-like growth factors in ErbB-3 binding specificity is derived from the observation that exchange of the linear N-terminal region of EGF by NRG-1 or TGF-α sequences results in chimeras, designated biregulin and T1E, respectively, that show high binding affinity not only for ErbB-1 but also for ErbB-2/ErbB-3 heterodimers (*8*, *15*). Notably, residues in the linear N-terminal region in EGF are not involved in ErbB-1 interaction (*15*). In contrast to NRG-1, however, these chimeras were unable to bind ErbB-3 alone, suggesting that a low-affinity interaction of these ligands with ErbB-3 is stabilized by subsequent binding of ErbB-2.

Essential for the activity of the ErbB signaling network is the ability to undergo ligand-induced receptor dimerization. ErbB-2 augments signaling through the ErbB network by acting as the preferred dimerization partner to the other members of the family (*16*−*18*), resulting in enhanced ligand binding affinity and a higher diversity in second messenger signaling (*19*−*21*). Particularly in the case of ErbB-3 heterodimer formation with ErbB-2 is essential, since ErbB-3 receptors have an impaired tyrosine kinase domain, and as a result ErbB-3 homodimers are biologically inactive (*22*, *23*). This mutual dependence makes the ErbB-2/ErbB-3 heterodimer a good model system to study ErbB receptor heterodimerization. Although the precise mechanism of ligand-induced ErbB dimerization is still unclear, it has been postulated that EGF-like growth factors may have a bivalent character and directly bridge two receptors into a dimeric complex (*24*−*26*).

To gain more insight into the manner of interaction between EGF-like ligands and heterodimeric ErbB-2/ErbB-3 receptors, we focused on the role of the linear N-terminal region in EGF for receptor binding. In a previous report we have shown that replacement of only two amino acids in the linear N-terminal region of EGF by their TGF-α equivalent (S2H and D3F) is sufficient to make EGF a high-affinity ligand for ErbB-2/ErbB-3 dimers (*8*). In addition, mutagenesis studies on NRG-1 have indicated the importance of Val4 (*14*). In the present study we have optimized the binding of EGF to ErbB-2/ErbB-3 heterodimers by random mutation of positions 2, 3, and 4[2] in the N-terminus using a phage display approach. Phage display has been shown to be a powerful technique to study receptor−ligand interactions, as it is an efficient method to rapidly select binders with enhanced affinity or altered selectivity to a target molecule (*27*). Variants with enhanced affinity to ErbB-2/ErbB-3 were selected by binding to MDA-MB-453 cells expressing ErbB-2 and ErbB-3 but which are devoid of ErbB-1. Functional characterization of the selected clones was obtained by binding and growth stimulation assays on 32D cells transfected with ErbB-2 and ErbB-3. Our data show that the EGF variants identified in this way show, unlike biregulin and T1E, high binding affinity not only for ErbB-2/ErbB-3 heterodimers but also for ErbB-3 alone. These data are interpreted in terms of the potential mechanism by which EGF-like growth factors mediate receptor binding.

EXPERIMENTAL PROCEDURES

Construction of the Human EGF/234 Library. A library of phage EGF randomly mutated at positions 2, 3, and 4 was constructed by a PCR-based approach using a degenerate oligonucleotide primer [forward primer, 5′-GCGGTACCG-GCCGACAANNSNNSNNSGAGTGTCCGTTGAGTCAC-GAC-3′; reverse primer, EGFback (*28*)] using fUSE5/hEGF as template. The PCR fragments were cloned into the phage fd fUSE5 vector (*29*) using the *Eag*I and *Sfi*I sites. Ligation products were electroporated into *Escherichia coli* TG-1 cells for phage production. The number of transformants was calculated and used to determine the size of the library. Randomly picked clones from the library were sequenced by cycle sequencing (Perkin-Elmer) to confirm diversity of codon use.

Cell Lines. Interleukin (IL) 3 dependent murine 32D hematopoietic progenitor cells transfected with the various human ErbB-encoding viral vectors or plasmids were cultured in RPMI-1640 medium supplemented with 10% heat-inactivated fetal calf serum (FCS, Gibco BRL, Paisley, Scotland) and 0.25 ng/mL mIL-3 (Promega, Madison, WI). The 32D sublines used, designated D1 (ErbB-1, 1.8 × 10^4 receptors/cell), D3 (ErbB-3, 1.1 × 10^4 receptors/cell), and D23 (ErbB-2 and ErbB-3, 1.3 × 10^4 ErbB-3 receptors/cell), were kept under continuous selection using 0.6 mg/mL G418 (Calbiochem, La Jolla, CA) and, in the case a second ErbB receptor was coexpressed, 0.4 mg/mL hygromycin B (Sigma, St. Louis, MO) as described (*30*). The human mammary

[2] Numbering according to human EGF.

carcinoma cell lines MDA-MB-453 and MCF-7S were cultured in a 1:1 mixture of Dulbecco's modified Eagle's medium and Ham's F12 medium (DF) supplemented with 10% FCS. Murine NIH-3T3 clone 2.2 cells devoid of endogenous ErbB receptors and two different NIH-3T3 clones transfected with hErbB-1, 2.2/HER and HER-14 cells (both 4.0×10^5 human ErbB-1 receptors/cell), were cultured in gelatinized flasks in Dulbecco's modified Eagle's medium (DMEM) supplemented with 10% newborn calf serum (*31*).

Preparation of Phage. Phage preparations were carried out as described (*32*). For ELISAs, small-scale phage preparations were used. Bacterial clones were grown at 30 °C in 1.5 mL of 2×TY medium containing 12.5 μg/mL tetracycline. To the culture was added supernatant polyethylene glycol (PEG) 8000 to precipitate the phages. Phages were finally resuspended in 100 μL of phosphate-buffered saline (PBS: 136 mM NaCl, 2 mM KCl, 10 mM Na_2HPO_4, 2 mM KH_2PO_4, pH 7.4), typically resulting in phage titers of $(1-5) \times 10^{10}$ tu/mL.

Selection on Cells in Suspension. The procedure for panning on whole cells in suspension was adapted from Watters et al. (*33*). MDA-MB-453 cells were harvested by trypsination, washed in PBS supplemented with 10% FCS, centrifuged for 4 min at 1200 rpm, resuspended in selection buffer [PBS supplemented with 0.1% bovine serum albumin (BSA), 1 mM $CaCl_2$, and 2 mM $MgCl_2$], and preincubated for 30 min at room temperature. Phage selections were carried out by incubation of 2×10^7 cells together with 3×10^8 phages of the EGF/234 library in 3 mL of selection buffer for 1 h at room temperature with gentle agitation. Unbound phages were removed by washing the cells 10 times with 10 mL of PBS containing 0.1% Tween 20 and by spinning the cells for 4 min at 1000 rpm followed by resuspension. Two subsequent washes were performed with PBS. During the washing procedure, cells were transferred twice to clean tubes to get rid of phages nonspecifically bound to the plastic. Cell-bound phages were harvested by 8 min incubation in acid elution buffer (0.1 M HCl/glycine, pH 2.2) followed by neutralization of the eluate by addition of an equal volume of 1 M Tris-HCl, pH 8.0. The eluate was transferred to an Eppendorf tube and spun for 5 min at 13000 rpm to eliminate cell debris, after which the supernatant was transferred to a fresh tube. Eluted fractions were used for phage titration and infection of logarithmic cultures of *E. coli* strain TG-1.

Whole Cell Phage ELISA. The procedure for ELISA using phage on whole cells in suspension was adapted from Hoogenboom et al. (*34*). Phage solutions were prepared in PBS/2% BSA. Cells were harvested, washed, and resuspended in phage-binding buffer (RPMI, 10 mM HEPES, 2% BSA). Cells were seeded in 96-well microtiter plates with V-shaped bottoms (Greiner 651101) at 1×10^6 cells per well in 0.15 mL and preincubated for 30 min at room temperature on a rowing boat shaker, after which they were spun for 4 min at 1000 rpm. Cell pellets were carefully resuspended in the phage mix. After incubation for 1 h at room temperature with gentle agitation, cells were spun for 4 min at 1000 rpm, after which the supernatant was removed and the cells were washed three times with 0.18 mL of PBS/well. For detection of cell-bound phage, cells were incubated for 1 h at room temperature with peroxidase-conjugated anti-M13 antibody in PBS/1% BSA (Pharmacia Biotech, Uppsala, Sweden). Cells were spun for 4 min at 1000 rpm and washed three times with PBS followed by addition of substrate, 0.1 mL of 0.4 mM 3,3′,5,5′-tetramethylbenzidine (Sigma, St. Louis, MO), and H_2O_2 in 0.11 M citrate buffer, pH 5.5. The reaction was terminated after 4 min by addition of 0.05 mL of 2 N H_2SO_4. Cells were spun for 4 min at 1000 rpm, and 0.12 mL of supernatant was transferred to a new 96-well plate. Absorption was read at 450 nm.

Construction and Production of Recombinant EGF/234 Mutants. Mutants EGF/WVS and EGF/WRS were constructed by introduction of the respective mutations in pEZZ/FX/EGF vector (*35*) using QuickChange site-directed mutagenesis (Stratagene, La Jolla, CA). The exact sequence was verified by cycle sequencing (Perkin-Elmer, Foster City, CA). Recombinant growth factors were expressed and purified as described (*35*). Briefly, mutant growth factors were expressed as protein A-tagged fusion proteins in the protease K-deficient *E. coli* strain KS474 and isolated from the periplasmic fraction. Growth factors were resolved by means of affinity chromatography using IgG−Sepharose, followed by factor X cleavage of the tag, an additional round of affinity chromatography to remove the protein A tag, and a final reverse-phase (RP) HPLC purification step. The amount of growth factor was calculated from the peak area (absorption at 229 nm) in the RP-HPLC chromatogram, using natural murine (m)EGF as a standard. The proper molecular sizes of EGF/WRS and EGF/WVS were verified by MALDI-TOF analysis.

Ligand Displacement Experiments. Natural mEGF (Bioproducts for Science Inc., Indianapolis, IN) and recombinant human NRG-1$\beta_{177-246}$ (R&D Systems, Minneapolis, MN) were radiolabeled using the Iodogen method (Pierce) according to the manufacturer's protocol for indirect labeling, resulting in a specific activity of 50−80 μCi/μg of protein. Binding displacement on HER-14 cells was performed as described (*35*). Ligand displacement analyses on 32D cells were performed using 1.5×10^6 D23 cells or 2×10^6 D3 cells as described (*30*). Cells were washed once with binding buffer (RPMI 1640 supplemented with 20 mM HEPES, pH 7.4, and 0.5% BSA) and subsequently incubated for 2 h at 4 °C with serial dilutions of unlabeled ligand in the presence of 1 ng/mL [^{125}I]NRG-1β. Cells were washed once with binding buffer and loaded onto a 0.6 mL serum cushion to remove the unbound label. Subsequently, cells were centrifuged at 2000 rpm, and cell surface-bound radioactivity was determined by γ-counting.

Cell Proliferation Assays. 32D cells were washed in RPMI 1640 medium to deprive them of IL-3. Subsequently, cells were seeded into 96-well tissue culture plates at a density of 5.0×10^4 cells/well in 0.1 mL of RPMI supplemented with 0.1% BSA, together with serial dilutions of filter-sterilized phages or recombinant growth factors. Cell survival was determined after 24 h of incubation at 37 °C using the 3-(4,5-dimethylthiazol-2-yl)-2,5-diphenyltetrazolium bromide (MTT) assay, as previously described (*30*).

Western Blotting. 32D cells were serum-starved for 2 h prior to stimulation. Cells were exposed to the indicated growth factors (100 ng/mL) for 7 min at 37 °C, rinsed three times with ice-cold PBS, and lysed in RIPA buffer containing freshly added protease inhibitors (50 mM Tris-HCl, pH 8.0, 150 mM NaCl, 1% NP-40, 0.5% sodium deoxycholate, 0.1% SDS, 1.5 mM EGTA, 1.5 mM $MgCl_2$, 1 mM PMSF, 5 μg/mL pepstatin A, 0.15 units/mL aprotinin, 5 μg/mL leupeptin,

2 mM Na_3VO_4). Lysates were cleared by centrifugation and resolved by SDS−polyacrylamide electrophoresis (SDS−PAGE) using 7.5% gels and electrophoretically transferred to nitrocellulose (Schleicher & Schuell, Germany). Membranes were incubated for 2 h in TBST (10 mM Tris-HCl, pH 7.5, 150 mM NaCl, and 0.05% Tween 20) containing 5% low fat milk, probed with 0.1 μg/mL anti-phosphotyrosine (Upstate Biotechnology Inc., Lake Saranac, NY), anti-EGFR 1005 or anti-ErbB-3 C17 (both from Santa Cruz Biotechnology, Santa Cruz, CA) antibodies for 2 h, washed twice with TBST, and subsequently incubated with a peroxidase-linked secondary antibody. Immunoreactive bands were visualized using enhanced chemiluminescence (ECL, Boehringer, Mannheim).

RESULTS

Construction of the EGF/234 Phage Library. To further elucidate the requirements for ErbB-3 binding and heterodimerization with ErbB-2, the linear N-terminal region of human EGF was randomized at positions Ser2, Asp3, and Ser4. An alignment of the sequences of human EGF, the EGF/TGF-α chimera T1E, and the EGF domain of human NRG-1β is given in Figure 1. In previous work we have shown that exchange of Ser2 and Asp3 of EGF for the corresponding His and Phe residues present in TGF-α results in a ligand with high affinity for ErbB-2/ErbB-3 heterodimers, indicating that amino acids at these positions are important for selective binding to this heterodimer (*8*). Moreover, studies on NRG-1 have identified Val4 as part of the binding domain to ErbB-3 (*14*, *15*). Therefore, we have constructed the EGF/234 library in which at positions 2, 3, and 4 all 20 amino acids were allowed, resulting in a complexity of 8.0×10^3 different amino acid combinations. The completeness of the library was estimated from the number of independent transformants (1.2×10^6), while sequencing of an aliquot of the phage library confirmed the genetic diversity and the expected amino acid distribution (data not shown).

Design of the Selection Procedure. To select EGF variants with improved binding affinity for ErbB-2/ErbB-3 heterodimers, we first generated a T1E phage to serve as a positive control in addition to the previously described EGF phage (*28*) as a negative control. T1E was displayed on pIII minor coat protein using the type 3 vector fUSE5. Both T1E phage and EGF phage bound well to NIH 3T3 cell clone 2.2 transfected with human ErbB-1 (2.2/HER) but not to untransfected parental cells (Figure 2), which is indicative for receptor-specific phage binding. T1E phage and EGF phage were also equally potent in ErbB-1 receptor activation (data not shown), as measured by the induction of luciferase activity in 2.2/HER cells transfected with an SIE-luciferase construct (*28*).

To find the best cell line for ErbB-2/ErbB-3 selection, several cell lines expressing ErbB-2 and ErbB-3 receptors were analyzed for selective binding of T1E phage versus EGF phage and control phage expressing a nonrelated protein, using an ELISA assay on cells in suspension (Figure 2). D23 cells, hematopoietic 32D cells lacking endogenous ErbB receptors transfected with both ErbB-2 and ErbB-3, were found to discriminate well between T1E and EGF phages. MCF-7 cells, which contain all four ErbB receptors

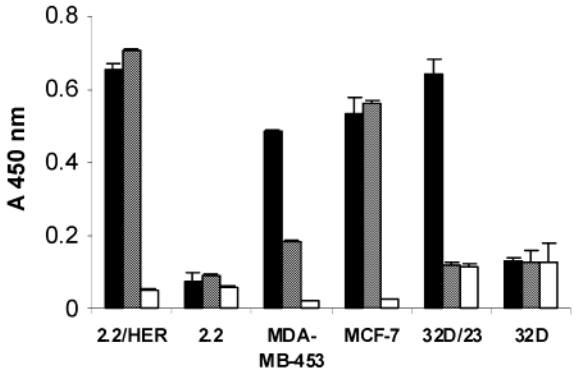

FIGURE 2: Whole cell ELISA of phage on cells expressing different ErbB receptors. Differential binding of T1E phage (black bars), EGF phage (hatched bars), and control phages (white bars) [$(2-4) \times 10^8$ tu/100 μL] was determined on clone 2.2 NIH3T3 fibroblasts and 2.2/HER cells (4×10^5 cells) or MDA-MB-453, MCF-7, 32D parental cells and 32D/23 cells expressing ErbB-2/ErbB-3 (2×10^6 cells). The amount of bound phage to cells in suspension was visualized by peroxidase-conjugated anti-M13 antibodies. Data represent the mean ± SD of two independent experiments performed in duplicate.

to a different extent, did not discriminate between binding of T1E and EGF phage. By contrast, MDA-MB-453 cells, which have high expression levels of ErbB-2 and ErbB-3 but have no detectable levels of ErbB-1 or ErbB-4, clearly favored binding of T1E phage over EGF phage. Thus, both D23 and MDA-MB-453 cells are appropriate candidates for selection of phages targeting ErbB-2/ErbB-3 receptors. To test the selection procedure for cells in suspension, these cell lines were next subjected to a mixture of T1E phage and negative control phages in a 1:1000 ratio, followed by washing and acid elution of bound phages. The D23 cells did not survive the extensive washing procedure, resulting in very low output levels. The MDA-MB-453 cells were found to select T1E phages well (~65% of eluted phages represented T1E phage, indicating >500-fold enrichment), and therefore, this cell line was used in the biopanning of the EGF/234 library. In addition, after selection individual phage clones were screened in an ELISA on 32D parental versus D23 cells to confirm specific ErbB-2/ErbB-3 binding.

Selection of EGF Variants on MDA-MB-453 Cells Expressing ErbB-2 and ErbB-3. The library of EGF/234 phages was subjected to three rounds of selection on MDA-MB-453 cells in suspension. After each selection round the pool of eluted phages was analyzed for ErbB-2/ErbB-3 binding in ELISAs on D23 cells. Already after the first selection round a clear improvement in binding was observed in comparison with the initial phage EGF/234 library, which is indicative for specific phage selection. Enrichment was also indicated by increased input/output ratios (data not shown).

After selection, individual phage clones were tested for specific ErbB-2/ErbB-3 binding by ELISAs on D23 cells versus parental 32D cells, and the sequence of clones able to bind ErbB-2/ErbB-3 was subsequently determined. Table 1 lists the sequence and the frequency of occurrence of the amino acid combinations on positions 2, 3, and 4 of the selected EGF variants. EGF variants were subdivided into a group of high-affinity binders ($n = 30$) and of intermediate binders ($n = 17$) according to the signal intensity in ELISAs

Table 1: Sequences of Selected EGF/234 Phage Variants Binding to ErbB-2/ErbB-3 Expressing Cells

EGF variant[a]	2 3 4	occurrence[b]	binding[c]	round[d]
group 1	**WRR**[e]	5	++	3
	WKR	2	++	2, 3
group 2	**WVR**[e]	5	++	2, 3
	WVK	1	++	3
	WIK	1	++	3
group 3	**WTR**[e]	6	++	2, 3
	WTK	1	+	3
	WGR	1	+	3
	HGR	1	+	2
group 4	**WVL**	1	++	2
	WLL	1	++	2
	WWV	1	+	3
	HVV	1	+	3
group 5	WRT	2	++	2, 3
	WRS	1	++	3
	WRG	2	++	2, 3
group 6	**WVS**	2	++	2
	WVG	2	+	3
	WVA	1	++	3
	HVA	1	+	3
	WIS	1	+	3
	WIA	2	+	3
	WLS	1	+	3
	HWS	1	+	2
miscellaneous	WMQ	1	+	3
	SWV	1	+	3
	HWE	1	+	2
	MTE	1	+	2

[a] EGF variants were grouped according to the type of residue (basic, hydrophobic, small) found at positions 3 and 4 in combination with Trp2 or His2 (see Figure 3B). EGF variants chosen as a representative clone for a given category are shown in bold face. [b] Total number of positive clones identified in phage ELISA ($n = 47$). [c] Clones were identified as intermediate (+) or high (++) affinity binders in phage ELISA on D23 cells in suspension. (+) Signal intensity ≥60% compared to T1E phage; (++) signal >80% compared to T1E phage. [d] Clones were isolated after two or three selection rounds on MDA-MB-453 cells. [e] Distinct codon use was observed for WRR (2), WVR (3), and WTR (2).

using T1E phage as a positive control. No exclusive convergence was observed after three rounds of selection, indicating that multiple substitutions in EGF result in enhanced ErbB-2/ErbB-3 binding. However, analysis of the occurrence of amino acids per position showed that 85% of the selected EGF variants contained Trp at position 2, while the remaining variants had predominantly a His residue (11%), indicating that an aromatic amino acid is preferred at this position (see Figure 3A). At position 3 mostly hydrophobic residues (43%), predominantly Val, were observed, although basic residues were also frequently found (26%). At position 4 the majority of clones contained a basic residue (49%), but also small residues such as Ser and Thr (19.1%) or Gly and Ala (14.9%) were regularly found. It is important to note that 60% of all selected clones contained at least one basic residue at position 3 or 4, which indicates that there is a selection in favor of a positively charged residue in this region, although the precise position seems of less importance. Relatively more His residues were found at position 2 in the intermediate binders (25%) in comparison with the high-affinity binders (3.3%). Intermediate binders also contained more small residues at positions 3 and 4 at the cost of basic residues. In general, the diversity of isolated clones was not clearly reduced in round 3 compared to the clones isolated in round 2.

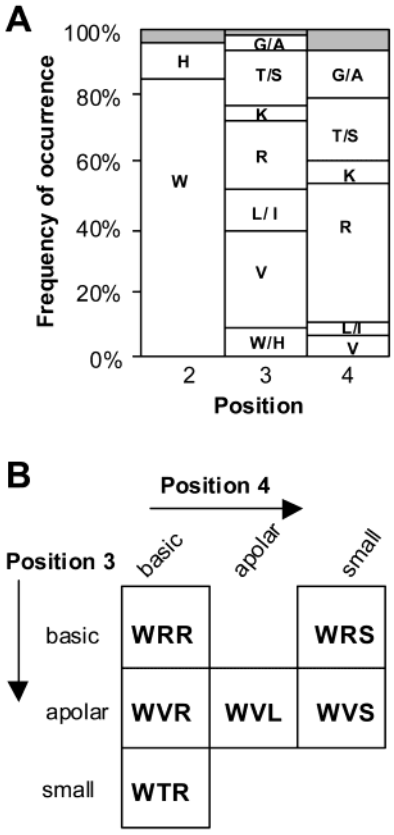

FIGURE 3: Schematic representation of the amino acid distribution in selected EGF/234 variants. (A) Frequency of occurrence of amino acids at positions 2, 3, and 4 in selected EGF variants. Both high and intermediate affinity binders, as determined in phage ELISAs on D23 cells, were used ($n = 47$). The gray area represents residues other than depicted (see Table 1). (B) Categorization of selected EGF variants according to the combination of amino acids found at positions 3 and 4, in addition to an aromatic (W or H) residue at position 2. The *y*-axis depicts the type of residue according to biochemical properties found at position 3 and the *x*-axis that at position 4. The indicated sequence corresponds to the most frequently observed EGF/234 variant, which was chosen as the representative variant for the given category.

Selected EGF Variants Fall into Six Categories. The selected EGF variants can basically be grouped in six categories according to the type of amino acid (basic, hydrophobic, small) found at positions 3 and 4, combined with Trp or His at position 2. Figure 3B depicts the most frequently observed sequences found in each category, hereafter referred to as representative clones. These data imply that selection occurred for distinct combinations of residues following the aromatic Trp2. A hydrophobic residue at position 4 was only observed in combination with a hydrophobic residue at position 3 (WVL), but not with a basic or small residue. In contrast, at position 4 a basic residue seems to be favored, independent of the residue present at position 3. The highest diversity of sequences was found in the category of the WVS type, although many clones in this group represent intermediate affinity binders. Interestingly, the corresponding sequences present in T1E (HFN) and EGF/S2H-D3F (HFS) were not observed. In conclusion, although many different sequences seem to confer ErbB-2/ErbB-3 binding, all selected sequences fit into a strict pattern of combinations of residues.

Mitogenic Potency of EGF Phage Variants Correlates with Their Binding. To assess the biological potency of the EGF

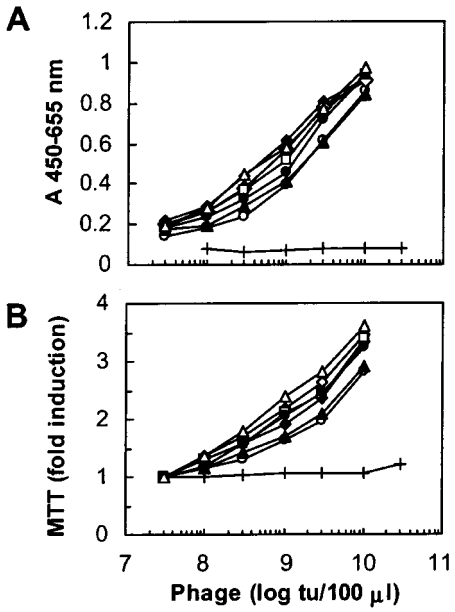

FIGURE 4: Comparison of cell binding and mitogenic activity of representative EGF variants on cells coexpressing ErbB-2 and ErbB-3. (A) Cell binding of the different representative EGF variants was measured in phage ELISA on D23 cells in suspension. (B) The potency of the representative EGF variants to induce proliferation of D23 cells was determined by the MTT assay, which measures mitochondrial activity in living cells. Cells were deprived of IL-3 and subsequently incubated at 37 °C in the absence or presence of serial dilutions of filter-sterilized phages for 24 h. In both experiments EGF phage and T1E phage served as controls. Key: phage EGF (+), T1E (○), EGF/WRR (◆), EGF/WVR (◇), EGF/WTR (□), EGF/WVL (▲), EGF/WRS (●), and EGF/WVS (△). Results of the MTT assay are presented as fold induction in treated cells versus untreated cells. Experiments were performed three times in duplicate, and a representative experiment is shown.

variants selected for enhanced ErbB-2/ErbB-3 binding, representative phage clones of each of the six categories were propagated on a larger scale. The titers of the PEG-purified and subsequently filter-sterilized phages were estimated on the basis of spectrometry, titration, and phage ELISA. Figure 4A depicts the binding of the representative EGF variants measured in ELISA on D23 cells in a dose−response experiment. Each of these phage clones bound D23 cells at least as well as T1E phage, with only slight differences between distinct EGF variants. Phage EGF served as a negative control. Next, the same phage clones were analyzed for the potential to induce proliferation of D23 cells using the MTT assay, which measures mitochondrial activity in living cells. The representative EGF variants showed enhanced mitogenic activity toward D23 cells in comparison with EGF phage and were all at least as potent as T1E phage. The mitogenic activity of the representative EGF variants on D23 cells corresponded in general well with their relative cell binding ability (Figure 4B). Thus, in a phage format selected EGF variants showed improved capacity to bind and activate ErbB-2/ErbB-3 heterodimers when compared to wild-type EGF.

Influence of Trp versus His Residues at Position 2 in EGF/234 Variants. Several EGF variants identified as intermediate binders were found to contain a His residue at position 2, while most high-affinity binders contain a Trp at this position. Remarkably, in the natural growth factors often His, but never Trp, is observed at the equivalent position. To examine

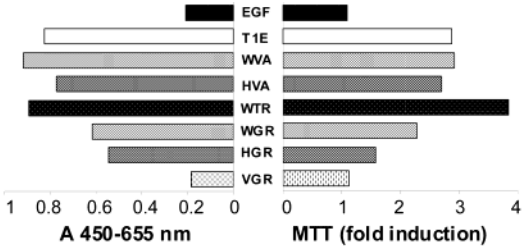

FIGURE 5: Comparison of cell binding and mitogenic activity of EGF variants containing either Trp or His residues at position 2. Left panel: Binding of distinct phage EGF variants to D23 cells was measured by ELISA on cells in suspension. Right panel: Ligand-induced proliferation of D23 cells by the same phage EGF variants was determined in the MTT assay after 24 h incubation. In both assays the concentration of phage used was 1×10^{10} tu. Experiments were performed two times in triplicate, and a representative experiment is shown.

whether the preference for Trp2 was due to true affinity enhancement and to exclude possible selection bias for Trp residues, we compared various phage clones which differed only in Trp or His at position 2 with respect to D23 cell binding and proliferation. Figure 5 shows that, at similar concentrations, variant EGF/WVA shows more cell binding (left panel) and mitogenic activity (right panel) on D23 cells than EGF/HVA, although the differences are relatively small. More pronounced differences were observed in the case of phage clone EGF/WGR, which was found superior to EGF/HGR in both cell binding and proliferation, while EGF/VGR failed to bind D23 cells and had a similar low activity as EGF phage. The representative clone of this category, EGF/WTR, exceeds EGF/WGR in binding and activation, suggesting that the most abundantly isolated clone represents the strongest binder within this category. Taken together, these data show that the abundant occurrence of Trp at position 2 in selected EGF/234 variants results directly from their enhanced affinity for ErbB-2/ErbB-3.

Characterization of Recombinant EGF Mutants for Binding to Distinct ErbB Receptors. Phage display of randomized EGF variants is a useful method to identify the sequences involved in selective ErbB-2/ErbB-3 binding, but it is inappropriate for the determination of accurate receptor binding affinity of the various variants. Since each phage may potentially display two to five copies of each ligand, multivalent receptor interactions may occur, resulting in an increased apparent affinity or avidity effect. Therefore, we have expressed two representative EGF variants as soluble recombinant proteins in *E. coli.* Since in the selected EGF variants the wild-type Ser4 residue was regularly observed, we focused on the contribution of Trp2 in combination with either Val3 or Arg3. The variants EGF/WVS and EGF/WRS, respectively, were further characterized as mutant proteins after RP-HPLC purification with respect to their relative binding affinities and mitogenic potencies to different ErbB receptors.

First, the recombinant EGF mutants were analyzed for ErbB-1 binding by displacement of [^{125}I]mEGF binding on HER-14 cells overexpressing human ErbB-1 receptors. Figure 6A shows that the ErbB-1 receptor binding capacity of EGF/WVS and EGF/WRS was completely retained in comparison with EGF and T1E. These data confirm previous observations that residues in the N-terminal linear region of EGF are not relevant for ErbB-1 interaction (*15*).

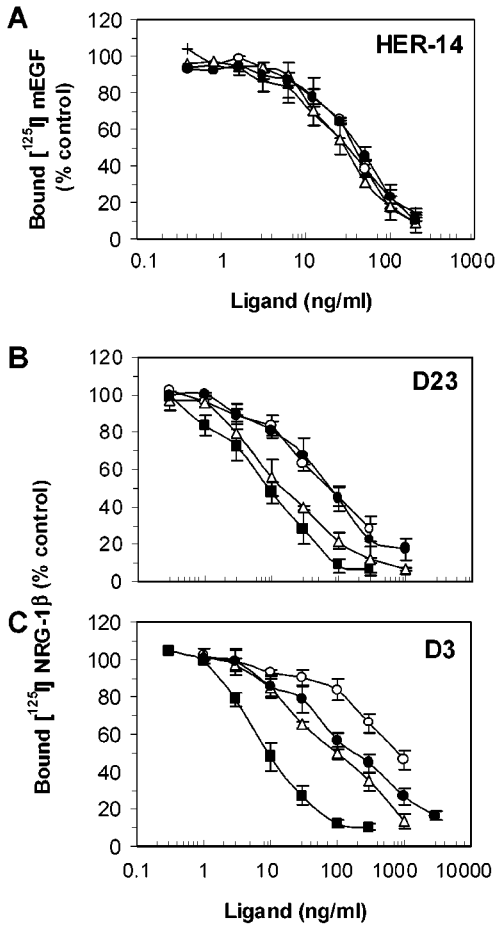

FIGURE 6: Ligand displacement analysis of recombinant EGF mutants on cells expressing different subsets of ErbB receptors. (A) Displacement of [^{125}I]mEGF binding on HER-14 cells expressing human ErbB-1. (B) Displacement of [^{125}I]hNRG-1β binding on 32D cells coexpressing ErbB-2 and ErbB-3 (D23 cells) or (C) on 32D cells expressing ErbB-3 alone (D3 cells). Cells were incubated for 2 h at 4 °C in the presence or absence of serial dilutions of the unlabeled ligands EGF (+), NRG-1β (■), T1E (○), EGF/WRS (●), or EGF/WVS (△). In case of the 32D cells, unbound ligand was removed by centrifugation of the cells through a serum cushion, after which radioactivity was determined in the cell pellet. Results are presented as mean ± SEM of at least three independent experiments performed in duplicate.

Second, the EGF mutants were analyzed for binding to ErbB-2/ErbB-3 expressing cells. Figure 6B shows the ability of the various ligands to compete with [^{125}I]NRG-1β binding to D23 cells. EGF/WRS showed similar relative binding affinity toward ErbB-2/ErbB-3 receptors as T1E, while the affinity of EGF/WVS was 5-fold higher than the affinity of T1E, nearly similar to NRG-1β. Wild-type EGF competed under these conditions only at concentrations above 500 ng/mL (*36*).

Third, the two EGF mutants were analyzed for binding to 32D cells expressing ErbB-3 alone (D3 cells). We have previously shown that T1E binds with high affinity to ErbB-2/ErbB-3 complexes but only weakly to the ErbB-3 receptor alone (*8*). A similar observation has been made for the NRG-1/EGF chimera biregulin (*25*). Interestingly, both EGF/WVS and EGF/WRS showed a 10-fold higher relative binding affinity than T1E in a competition experiment with [^{125}I]-NRG-1β on D3 cells, with an apparent affinity 10-fold lower than that of NRG-1β (Figure 6C). Taken together, these data indicate that the substitution of WVS and WRS into EGF specifically enhances the binding affinity for ErbB-3, leaving the ErbB-1 binding unaffected. This results in ligands that not only strongly bind to ErbB-1 and ErbB-2/ErbB-3 receptors but also bind to ErbB-3 alone.

Mitogenic Activity of Recombinant EGF Mutants through Distinct ErbB Receptors. Finally, the EGF mutants were analyzed for the ability to activate distinct ErbB receptors by measuring both ligand-induced tyrosine phosphorylation and the mitogenic activity in 32D cells expressing specific ErbB receptor members. Panels A and C of Figure 7 show that EGF/WVS and EGF/WRS are equally potent inducers of tyrosine phosphorylation of the ErbB-1 receptor in 32D cells transfected with ErbB-1 (D1 cells). In addition, both mutants resembled wild-type EGF in inducing proliferation of D1 cells. Next, the activation of ErbB-2/ErbB-3 heterodimers was examined by measuring tyrosine phosphorylation of ErbB-2 and ErbB-3 receptors in whole cell lysates of D23 cells. As shown in Figure 7D, EGF/WVS was similarly potent as NRG-1β in inducing receptor tyrosine phosphorylation of D23 cells, while EGF/WRS and T1E were slightly less active. The same order of potencies was observed in a mitogenic assay on D23 cells, where EGF/WVS was also a stronger mitogen than EGF/WRS (Figure 7B). These data show that potent receptor activation and cellular stimulation parallel the high relative binding affinity of the two selected EGF variants for ErbB-2/ErbB-3 heterodimers.

DISCUSSION

To understand the selectivity of ligand binding to different members of the ErbB receptor family, we have studied the role of the linear N-terminal region of EGF-like ligands for interaction with ErbB-2/ErbB-3 heterodimers. In a previous study we have shown that exchange of the linear N-terminal region of EGF for TGF-α sequences results in a ligand (T1E) with high affinity for ErbB-2/ErbB-3 heterodimers but low affinity for ErbB-3 alone. Similar results were obtained with a ligand in which only two amino acids of TGF-α (S2H and D3F) were incorporated into EGF (*8*). In the current study we have used a phage display approach to optimize the binding of EGF to ErbB-2/ErbB-3 heterodimers by random mutation of the residues at positions 2, 3, and 4. Using whole cell selection several EGF variants with strong ErbB-2/ErbB-3 binding capacity were obtained, leading to a clear view of the sequence determinants that convert receptor specificity of EGF. Moreover, our results demonstrate that the selected EGF clones result in ligands that have increased affinity not only for ErbB-2/ErbB-3 heterodimers but also for ErbB-3 alone.

Comparison of the NMR solution and crystal structures reveals that the N-terminal linear region of human EGF is completely flexible, while in NRG-1α it forms the third strand of a triple β-sheet with the B-loop (*6*, *7*, *13*, *37*, *38*). TGF-α has a slightly more structured N-terminus than EGF (*39*). In the structure of NRG-1α two patches of hydrophobic and positively charged residues are exposed on opposite sites of the major triple β-sheet (*13*). One of these hydrophobic clusters of residues comprising Leu3, Phe21, Val23, and Leu33 has been implicated for ErbB-3 binding in an alanine scanning mutagenesis study, suggesting it may form the ErbB-3 binding site, although also mutation of residues in other regions affected the binding capacity (*14*). Our results

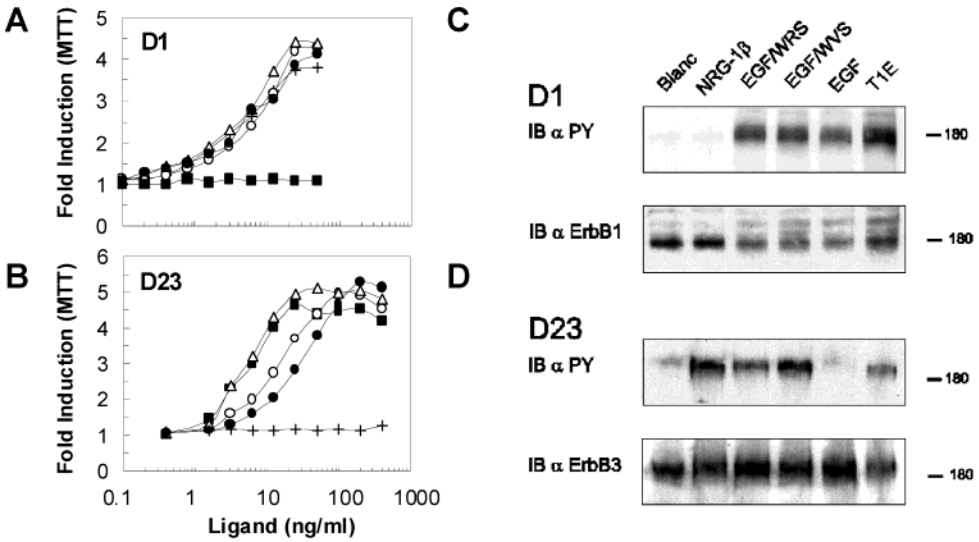

FIGURE 7: Activation of different ErbB receptor members by recombinant EGF mutants. (A, B) Induction of cell proliferation of 32D cells expressing ErbB-1 (D1 cells) and D23 cells by EGF (+), NRG-1β (■), T1E (○), EGF/WVS (△), or EGF/WRS (●) as measured in a MTT assay after 24 h. Data points represent the average of two experiments performed in duplicate. (C, D) Induction of tyrosine phosphorylation in D1 cells or D23 cells after stimulation for 7 min at 37 °C with the indicated ligands at 100 ng/mL determined by immunoblotting (IB) with anti-phosphotyrosine (PY) antibodies following SDS−PAGE of whole cell lysates. Western blots were reprobed after stripping with anti-ErbB-1 or anti-ErbB-3 antibodies. The 180 kDa marker protein is indicated.

subscribe to the idea that sequences in the N-terminal linear region directly participate in ErbB-3 receptor binding. In case the N-terminus is improved for ErbB-3 binding, as in EGF/WVS and EGF/WRS, these ligands are capable of forming both ErbB-3 homodimers and ErbB-2/ErbB-3 heterodimers. In case the N-terminal sequences are suboptimal for ErbB-3 binding, as in the chimeras T1E (HFN) and biregulin (HLV), the weak ErbB-3 binding can nevertheless be stabilized by subsequent heterodimer formation with ErbB-2. Previously, Tzahar and co-workers (*25*) postulated that NRG-1β contains two separate binding sites for two receptors, including a specific, high-affinity binding site for ErbB-3 and a broad specific, low-affinity binding site for another ErbB member such as ErbB-2. If EGF-like growth factors indeed may be bivalent ligands, this would imply that T1E and biregulin should contain a good secondary binding site for ErbB-2 but not for ErbB-3. In contrast, the improved primary ErbB-3 binding site of the EGF/WVS and EGF/WRS mutants in combination with the poor secondary binding site for ErbB-3 may already be sufficient to stabilize the dimer, although dimerization with ErbB-2 still seems preferred.

Phage display has been shown to be a powerful technique to achieve altered selectivity or enhanced binding for target molecules after randomization of ligand epitopes (*27*, *40*−*42*) and has been applied successfully for binding optimization of EGF-like growth factors (*43*−*45*). Moreover, selection of phage libraries performed on cell surface-expressed receptors has the advantage that the natural conformation is conserved, although other reports also described successful selection using purified receptor molecules (*45*, *46*). The most prominent amino acid residue present in the isolated EGF-variants with ErbB-2/ErbB-3 binding capacity was the Trp residue at position 2, implying that this residue is mainly responsible for the gain in binding affinity. In a phage display study for optimization of NRG-1β binding to ErbB-3-IgG fusion proteins, Trp was exclusively found at position 1 in the randomized N-terminus, in combination with different hydrophilic residues at position 2 (*45*). Since the Trp residue is located at the signal peptide cleavage site, the authors could not exclude the possibility of expression bias. The enrichment for Trp residues could also result from a length requirement to extend beyond a possible steric inhibition of the pIII molecule. However, these arguments do not seem relevant for the present study, since the fUSE5 vector used here contained an N-terminal extension of three residues between the signal peptide cleavage site and the ligand, which makes the possibility of a phage artifact unlikely. The observation that a Trp residue is abundantly recruited at position 2 of EGF therefore most likely indicates that this aromatic residue strongly enhances ErbB-3 binding.

In the selected EGF variants hydrophobic residues were particularly abundant at position 3, in agreement with the presence of Leu in NRG-1 and Phe in the chimera T1E. However, the frequent occurrence of basic residues (WRR and WRS categories) indicates that there is no absolute need for hydrophobicity at this position. This suggests that the presence of Trp2 may already provide sufficient hydrophobic packing. On the other hand, the difference in binding affinity between the WVS and WRS mutants indicates that the additional hydrophobicity derived from Val3 results in higher affinity to ErbB-2/ErbB-3. Residues with a hydrophilic character, either the basic Arg or small hydrophilic Ser and Thr, seem to be preferred at position 4. In contrast, in randomized NRG-1 selected for binding to ErbB-3−IgG fusion proteins the hydrophobic residues were predominantly found at postions 3 (Leu) and 4 (Val) (*45*). Interestingly, in the present study EGF variants with hydrophobic residues at position 4 (WVL category) were found in only 4 out of 47 clones. Taken together, our results indicate that, for optimal binding to ErbB-2/ErbB-3 receptors, EGF should preferentially contain an aromatic, a hydrophobic, and a positively charged amino acid at its positions 2, 3, and 4, although the exact position of these distinct residues may not be very strict.

Since the N-terminal linear region of EGF is unstructured, while in NRG-1 it forms a β-strand, the selected sequences

may very well reflect a structural requirement for ligand binding to ErbB-3. This is in agreement with the observation that substitutions in the N-terminus of EGF selectively affect ErbB-3 but not ErbB-1 binding. Besides having a function in direct receptor interaction, selected hydrophobic and aromatic residues in the N-terminus might contribute to hydrophobic packing with residues in the B-loop of EGF. The selected EGF variants are enriched for β-branched amino acids such as Thr and Val, and for amino acids with a tendency to support β-strand formation, as expressed in the Chou−Fasman algorithm (*47*). For instance, at each position Trp was preferred above His, Thr above Ser, and Arg above Lys. This suggests that the selected sequences may also favor stabilization of the N-terminal linear region of EGF into a β-strand as a structural requirement for EGF-like growth factors to bind ErbB-3. Determination of the NMR solution structure of T1E or any of the EGF variants selected here should reveal whether the proposed enhanced stabilization of the N-terminal linear region has indeed occurred.

When comparing the present results with those on optimization of NRG-1β binding to ErbB-3 (*45*), it should be realized that the studies have been carried out in an entirely different background of adjacent amino acids. By random mutation of only positions 2, 3, and 4, compensatory sequences can be selected that are not relevant for other ligand molecules. For instance, the presence of basic residues in 60% of all selected EGF variants at either position 3 or position 4 could be due to compensation of the presence of the acidic Asp5 in EGF, whereas NRG-1 contains a basic residue Lys5. Alternatively, since the B-loop of NRG-1 is enriched for basic residues (Lys24, Arg31, Lys35) in comparison with EGF (Lys28), the selected basic residues may compensate for the lack of positive charge in the adjacent B-loop. The importance of the local structure for receptor interaction is also illustrated by the report that exchange of the linear N-terminal region of NRG-1α with TGF-α sequences strongly impaired the ability to bind ErbB-2/ErbB-3, while introduction of similar sequences into EGF (T1E) strongly enhanced this ability (*8*, *48*). In comparison with EGF, the B-loop of NRG-1 is extended by three residues, which form an irregular Ω-loop. It would be interesting to study whether the presence of the Ω-loop plays a role in this controversy. Recently, it has been shown that a chimera in which the linear N-terminal region of NRG-1 is introduced into TGF-α is unable to activate ErbB-2/ErbB-3 heterodimers, thus emphasizing the importance of the presence of appropriate amino acids in the B-loop region (*49*).

The present data indicate that a Trp residue in the N-terminal linear region of EGF-like growth factors strongly enhances the binding affinity for ErbB-3. It is therefore intriguing that most natural ErbB-3 binding ligands have the less efficient His residue at this position. Among them are NRG-1 (residues HLV), NRG-2 (residues HAR), and the viral Shope fibroma growth factor (residues HVK) but also the ErbB-1 binding ligands TGF-α (residues HFN) and betacellulin (residues HFS) (*8*, *15*, *36*, *50*−*52*). Notably, Myxoma growth factor with the sequence RIK at these positions has been reported as a selective activator of ErbB-2/ErbB-3 heterodimers (*50*). This suggests that natural ligands are not necessarily optimized for high binding affinity to their receptor. This is also indicated by the observation that a high-affinity ligand such as NRG-1β could be further optimized more than 50-fold for ErbB-3 binding (*45*). Data from our group (unpublished results) and others (*53*) indicated that the mitogenic activity of EGF for ErbB-1-containing cells is limited by internalization and degradation of the receptor−ligand complex before cells are triggered to enter the S-phase. As a consequence, EGF mutants with a lower affinity for ErbB-1 were found to be at least as mitogenic as EGF itself. This suggests that an intermediate binding affinity coupled to strict receptor selectivity is most appropriate for the biological activity of natural ligands, especially under conditions where multiple ErbB members are coexpressed. EGF-like growth factors are also widely used to target toxins or other drugs to cells overexpressing ErbB receptors (*54*, *55*). The present observation that EGF with only two mutations (S2W, D3V/R) is a high-affinity ligand for ErbB-1, ErbB-3, and ErbB-2/ErbB-3 heterodimers makes this type of pan-ErbB ligands interesting candidates for targeting toxins to cells which overexpress multiple ErbB receptors, such as most human breast cancer cells.

ACKNOWLEDGMENT

We thank Mylène Weill, in whose laboratory the phage work was initiated, as well as Jérôme Gracy, Laurent Chiche, and Miriam Wingens for valuable discussions. Elmar Krieger is thanked for help with Figure 1.

REFERENCES

1. Yokota, J., Yamamoto, T., Toyoshima, K., Terada, M., Sugimura, T., Battifora, H., and Cline, M. J. (1986) *Lancet 1*, 765−767.
2. Hynes, N. E., and Stern, D. F. (1994) *Biochim. Biophys. Acta 1198*, 165−184.
3. Alroy, I., and Yarden, Y. (1997) *FEBS Lett. 410*, 83−86.
4. Riese, D. J., II, and Stern, D. F. (1998) *BioEssays 20*, 41−48.
5. Harari, D., Tzahar, E., Romano, J., Shelly, M., Pierce, J. H., Andrews, G. C., and Yarden, Y. (1999) *Oncogene 18*, 2681−2689.
6. Hommel, U., Harvey, T. S., Driscoll, P. C., and Campbell, I. D. (1992) *J. Mol. Biol. 227*, 271−282.
7. Lu, H. S., Chai, J. J., Li, M., Huang, B. R., He, C. H., and Bi, R. C. (2001) *J. Biol. Chem. 276*, 34913−34917.
8. Stortelers, C., Lenferink, A. E., van de Poll, M. L., Gadellaa, M., van Zoelen, C., and van Zoelen, E. J. (2002) *Biochemistry 41*, 4292−4301.
9. Groenen, L. C., Nice, E. C., and Burgess, A. W. (1994) *Growth Factors 11*, 235−257.
10. Campion, S. R., and Niyogi, S. K. (1994) *Prog. Nucleic Acid Res. Mol. Biol. 49*, 353−383.
11. Nandagopal, K., Tadaki, D. K., Lamerdin, J. A., Serpersu, E. H., and Niyogi, S. K. (1996) *Protein Eng. 9*, 781−788.
12. Nandagopal, K., Terzaghi-Howe, M., and Niyogi, S. K. (1999) *J. Cell. Biochem. 72*, 16−24.
13. Jacobsen, N. E., Abadi, N., Sliwkowski, M. X., Reilly, D., Skelton, N. J., and Fairbrother, W. J. (1996) *Biochemistry 35*, 3402−3417.
14. Jones, J. T., Ballinger, M. D., Pisacane, P. I., Lofgren, J. A., Fitzpatrick, V. D., Fairbrother, W. J., Wells, J. A., and Sliwkowski, M. X. (1998) *J. Biol. Chem. 273*, 11667−11674.
15. Barbacci, E. G., Guarino, B. C., Stroh, J. G., Singleton, D. H., Rosnack, K. J., Moyer, J. D., and Andrews, G. C. (1995) *J. Biol. Chem. 270*, 9585−9589.
16. Graus-Porta, D., Beerli, R. R., Daly, J. M., and Hynes, N. E. (1997) *EMBO J. 16*, 1647−1655.
17. Riese, D. J., II, van Raaij, T. M., Plowman, G. D., Andrews, G. C., and Stern, D. F. (1995) *Mol. Cell. Biol. 15*, 5770−5776.
18. Tzahar, E., Waterman, H., Chen, X., Levkowitz, G., Karunagaran, D., Lavi, S., Ratzkin, B. J., and Yarden, Y. (1996) *Mol. Cell. Biol. 16*, 5276−5287.
19. Wallasch, C., Weiss, F. U., Niederfellner, G., Jallal, B., Issing, W., and Ullrich, A. (1995) *EMBO J. 14*, 4267−4275.

20. Karunagaran, D., Tzahar, E., Beerli, R. R., Chen, X., Graus-Porta, D., Ratzkin, B. J., Seger, R., Hynes, N. E., and Yarden, Y. (1996) *EMBO J. 15*, 254−264.
21. Fitzpatrick, V. D., Pisacane, P. I., Vandlen, R. L., and Sliwkowski, M. X. (1998) *FEBS Lett. 431*, 102−106.
22. Guy, P. M., Platko, J. V., Cantley, L. C., Cerione, R. A., and Carraway, K. L., III (1994) *Proc. Natl. Acad. Sci. U.S.A. 91*, 8132−8136.
23. Sliwkowski, M. X., Schaefer, G., Akita, R. W., Lofgren, J. A., Fitzpatrick, V. D., Nuijens, A., Fendly, B. M., Cerione, R. A., Vandlen, R. L., and Carraway, K. L., III (1994) *J. Biol. Chem. 269*, 14661−14665.
24. Gullick, W. J. (1994) *Eur. J. Cancer 30A*, 2186.
25. Tzahar, E., Pinkas-Kramarski, R., Moyer, J. D., Klapper, L. N., Alroy, I., Levkowitz, G., Shelly, M., Henis, S., Eisenstein, M., Ratzkin, B. J., Sela, M., Andrews, G. C., and Yarden, Y. (1997) *EMBO J. 16*, 4938−4950.
26. Lemmon, M. A., Bu, Z., Ladbury, J. E., Zhou, M., Pinchasi, D., Lax, I., Engelman, D. M., and Schlessinger, J. (1997) *EMBO J. 16*, 281−294.
27. Smith, G. P., and Scott, J. K. (1993) *Methods Enzymol. 217*, 228−257.
28. Souriau, C., Fort, P., Roux, P., Hartley, O., Lefranc, M. P., and Weill, M. (1997) *Nucleic Acids Res. 25*, 1585−1590.
29. Scott, J. K., and Smith, G. P. (1990) *Science 249*, 386−390.
30. Pinkas-Kramarski, R., Shelly, M., Glathe, S., Ratzkin, B. J., and Yarden, Y. (1996) *J. Biol. Chem. 271*, 19029−19032.
31. Honegger, A. M., Szapary, D., Schmidt, A., Lyall, R., Van Obberghen, E., Dull, T. J., Ullrich, A., and Schlessinger, J. (1987) *Mol. Cell. Biol. 7*, 4568−4571.
32. Griffiths, A. D., and Duncan, A. R. (1998) *Curr. Opin. Biotechnol. 9*, 102−108.
33. Watters, J. M., Telleman, P., and Junghans, R. P. (1997) *Immunotechnology 3*, 21−29.
34. Hoogenboom, H. R., Lutgerink, J. T., Pelsers, M. M., Rousch, M. J., Coote, J., Van Neer, N., De Bruine, A., Van Nieuwenhoven, F. A., Glatz, J. F., and Arends, J. W. (1999) *Eur. J. Biochem. 260*, 774−784.
35. van de Poll, M. L., Lenferink, A. E., van Vugt, M. J., Jacobs, J. J., Janssen, J. W., Joldersma, M., and van Zoelen, E. J. (1995) *J. Biol. Chem. 270*, 22337−22343.
36. Pinkas-Kramarski, R., Lenferink, A. E., Bacus, S. S., Lyass, L., van de Poll, M. L., Klapper, L. N., Tzahar, E., Sela, M., van Zoelen, E. J., and Yarden, Y. (1998) *Oncogene 16*, 1249−1258.
37. Kohda, D., and Inagaki, F. (1992) *Biochemistry 31*, 11928−11939.
38. Nagata, K., Kohda, D., Hatanaka, H., Ichikawa, S., Matsuda, S., Yamamoto, T., Suzuki, A., and Inagaki, F. (1994) *EMBO J. 13*, 3517−3523.
39. Moy, F. J., Li, Y. C., Rauenbuehler, P., Winkler, M. E., Scheraga, H. A., and Montelione, G. T. (1993) *Biochemistry 32*, 7334−7353.
40. Wrighton, N., and Gearing, D. (1999) *Nat. Biotechnol. 17*, 1157−1158.
41. Lowman, H. B., Bass, S. H., Simpson, N., and Wells, J. A. (1991) *Biochemistry 30*, 10832−10838.
42. Lowman, H. B., and Wells, J. A. (1993) *J. Mol. Biol. 234*, 564−578.
43. Tang, X. B., Dallaire, P., Hoyt, D. W., Sykes, B. D., O'Connor-McCourt, M., and Malcolm, B. A. (1997) *J. Biochem. (Tokyo) 122*, 686−690.
44. Souriau, C., Gracy, J., Chiche, L., and Weill, M. (1999) *Biol. Chem. 380*, 451−458.
45. Ballinger, M. D., Jones, J. T., Lofgren, J. A., Fairbrother, W. J., Akita, R. W., Sliwkowski, M. X., and Wells, J. A. (1998) *J. Biol. Chem. 273*, 11675−11684.
46. Wrighton, N. C., Farrell, F. X., Chang, R., Kashyap, A. K., Barbone, F. P., Mulcahy, L. S., Johnson, D. L., Barrett, R. W., Jolliffe, L. K., and Dower, W. J. (1996) *Science 273*, 458−464.
47. Chou, P. Y., and Fasman, G. D. (1974) *Biochemistry 13*, 211−222.
48. Harris, A., Adler, M., Brink, J., Lin, R., Foehr, M., Ferrer, M., Langton-Webster, B. C., Harkins, R. N., and Thompson, S. A. (1998) *Biochem. Biophys. Res. Commun. 251*, 220−224.
49. Schmidt, M., and Wels, W. (2002) *Int. J. Cancer 97*, 349−356.
50. Tzahar, E., Moyer, J. D., Waterman, H., Barbacci, E. G., Bao, J., Levkowitz, G., Shelly, M., Strano, S., Pinkas-Kramarski, R., Pierce, J. H., Andrews, G. C., and Yarden, Y. (1998) *EMBO J. 17*, 5948−5963.
51. Alimandi, M., Wang, L. M., Bottaro, D., Lee, C. C., Kuo, A., Frankel, M., Fedi, P., Tang, C., Lippman, M., and Pierce, J. H. (1997) *EMBO J. 16*, 5608−5617.
52. Pinkas-Kramarski, R., Shelly, M., Guarino, B. C., Wang, L. M., Lyass, L., Alroy, I., Alimandi, M., Kuo, A., Moyer, J. D., Lavi, S., Eisenstein, M., Ratzkin, B. J., Seger, R., Bacus, S. S., Pierce, J. H., Andrews, G. C., Yarden, Y., and Alamandi, M. (1998) *Mol. Cell. Biol. 18*, 6090−6101.
53. Reddy, C. C., Niyogi, S. K., Wells, A., Wiley, H. S., and Lauffenburger, D. A. (1996) *Nat. Biotechnol. 14*, 1696−1699.
54. Landgraf, R., Pegram, M., Slamon, D. J., and Eisenberg, D. (1998) *Biochemistry 37*, 3220−3228.
55. Kirschbaum, M. H., and Yarden, Y. (2000) *J. Cell. Biochem. 77*, 52−60.

BI025878C